Proc. Natl. Acad. Sci. USA
Vol. 81, pp. 233–237, January 1984
Medical Sciences

Simple finite-element model accounts for wide range of cardiac dysrhythmias

(electrophysiology/computer simulation/dispersion of refractoriness/ventricular fibrillation)

JOSEPH M. SMITH* AND RICHARD J. COHEN*†

*Harvard–Massachusetts Institute of Technology Division of Health Sciences and Technology and †Department of Physics, Massachusetts Institute of Technology, Cambridge, MA 02139

Communicated by George B. Benedek, August 29, 1983

ABSTRACT **A simple finite-element model of ventricular conduction processes that explicitly incorporates spatial dispersion of refractoriness was developed. This model revealed that spatial dispersion of refractoriness is a sufficient condition to produce self-sustained reentry even in the absence of unidirectional block, inhomogeneity in local conduction velocities, or the presence of ectopic pacemakers. The model displayed a wide variety of rhythm disturbances qualitatively similar to clinically familiar cardiac dysrhythmias. Electrical stability of the model was determined as a function of the model parameters including ventricular stimulation rate, conduction velocity, and mean refractory period as well as standard deviation of refractory periods. We conclude that spatial dispersion of refractoriness is a sufficient condition to initiate reentrant dysrhythmias but that other physiologic variables such as ventricular rate and conduction velocity strongly influence the dysrhythmogenic effect of spatial dispersion of refractoriness.**

Over the past 20 years, a unified hypothesis concerning the mechanism of reentrant cardiac rhythm disturbances has been developed (1–4). The "dispersion of refractoriness" hypothesis is rooted in the concept that the spread of depolarization over myocardial tissue is fundamentally a synchronous process in which activation of one region of tissue spreads to activate neighboring regions. The process of repolarization, on the other hand, is fundamentally an asynchronous process in which local clocks determine the length of time during which a region of tissue remains depolarized and thus refractory to further stimulation. Spatial variation in refractory times leads to the appearance of islands of refractory tissue during the repolarization process (Fig. 1). A new wave of depolarization impinging on these islands of refractory tissue will fractionate. Such fractionation of the depolarization wave front can lead to eddies and reentry. These processes can lead to a variety of disturbances of heart rhythm, including single or multiple premature depolarizations, sustained tachydysrhythmias, and, ultimately, fibrillation. Fibrillation represents a completely chaotic turbulent pattern of local reentrant activity.

One may generalize the dispersion of refractoriness hypothesis to include not only spatial dispersion of refractory times but all factors that predispose to variability in the spatial coherence and temporal synchronization of the repolarization process. Variations in the local electrical properties of the myocardium (e.g., refractory period, conduction velocity) will predispose to "spatiotemporal dispersion of refractoriness" and, thus, to reentry.

This hypothesis is attractive in that it provides a simple conceptual basis for understanding a wide range of observations regarding factors that predispose or provoke reentrant cardiac dysrhythmias including fibrillation. For example, electrical stimulation of the ventricular myocardium during the "vulnerable period," which roughly corresponds in time to the peak of the T wave of the electrocardiogram (ECG), can provoke fibrillation even in a normal heart. The amplitude of the current pulse needed to just initiate fibrillation in fact provides a measure of the electrical stability of the ventricular myocardium and is referred to as the ventricular fibrillation threshold (5). The vulnerable period, according to the dispersion of refractoriness hypothesis, coincides with the peak of the T wave because this is the point in time during which roughly half of the cells are refractory and half are excitable—thus, this is the time when maximum fractionation of a new depolarization wave front should occur.

Diverse conditions such as hypothermia, β-sympathetic stimulation, coronary atherosclerosis in the absence of infarction, and myocardial ischemia all predispose to fibrillation. The mechanism by which these diverse conditions predispose to reentry may be understood in terms of their spatially inhomogeneous effects on the local electrical properties of the ventricular myocardium (1, 3, 4). Furthermore, the effect of tachycardia (even in the absence of β-sympathetic stimulation) in predisposing to fibrillation can be understood in terms of the depolarization wave front being initiated when a greater proportion of the myocardium is still refractory.

In addition, the profibrillatory effects of slow conduction and increased cardiac dimension (6, 7) can be understood by considering Fig. 2. Here we see that, for a reentrant path to be self-sustaining, the tissue at a given point along the path must no longer be refractory when the reentrant wave of depolarization returns. This consideration leads to a rough quantitative criteria for reentry

$$l > v\tau, \qquad [1]$$

where l is the loop circumference, v is the characteristic conduction velocity, and τ is the characteristic refractory time. A decrease in the mean conduction velocity decreases the right-hand side of this inequality and thus predisposes to self-sustained reentry. It is easier to pack a loop of fixed circumference in a large heart than in a small heart. Thus, it is easier to initiate ventricular fibrillation in a dog's heart than in a rat's heart.

Although the dispersion of refractoriness hypothesis has gained much support in recent years, with several authors reporting an increase in the variance of measured refractory periods in animal preparations subject to dysrhythmogenic conditions (8, 9), a quantitative test of the concept that dispersion of refractoriness is in fact a sufficient condition to produce a wide variety of cardiac rhythm disturbances is still lacking. A definitive test of this hypothesis in an animal preparation is not feasible. An alternative approach, and one that allows for gaining additional insight into basic mecha-

The publication costs of this article were defrayed in part by page charge payment. This article must therefore be hereby marked "*advertisement*" in accordance with 18 U.S.C. §1734 solely to indicate this fact.

Abbreviation: ECG, electrocardiogram.

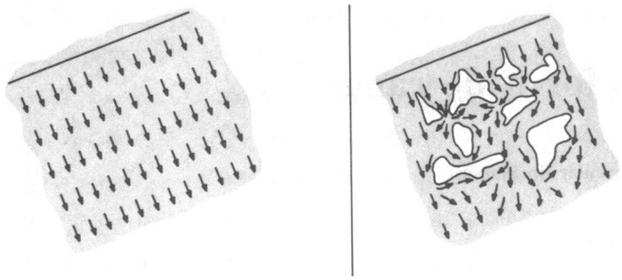

FIG. 1. Spatial homogeneity (*Left*) results in even spreading of depolarization wave. Spatial inhomogeneity in refractory times (*Right*) leads to wave-front fractionation and reentry. Unshaded regions represent islands of refractory tissue.

nisms, is to construct a simple computer model of ventricular conduction processes that explicitly incorporates spatial dispersion of refractoriness. The goal of this approach is not necessarily to develop a model that closely represents the detailed electrophysiology of ventricular conduction but rather to develop the simplest possible model that retains the key features of the problem and explicitly includes spatial dispersion of refractory times. The pioneering work of Moe *et al.* (10) represented an initial effort in this direction. Here we present an examination of the dynamic properties of such a simple finite model.

METHODS

The finite element model for ventricular conduction processes is depicted in Fig. 3. A cylindrical shell model was taken as a first-order approximation to ventricular geometry. The cylinder had a length (L) to diameter (D) ratio of 2 and was constructed from an array of square elements of linear dimension ξ. ξ physically represents the spatial length over which refractory tissues are correlated. ξ is a macroscopic distance typically of the order of 1 mm in our simulations. The total number of elements (N) was fully determined by the quantities L, the L/D ratio of 2, and the element dimension ξ. The typical number of elements was of the order of a few thousand.

Each element was allowed to be in one of only two states—repolarized (susceptible to stimulation) or depolarized (refractory to stimulation). Once an element depolarized it remained in that state for the duration of its preassigned refractory time. The τ values were randomly assigned to each element according to a Gaussian probability distribution with mean refractory time ($\bar{\tau}$) and standard deviation σ (the distribution was truncated at $\tau = 0$). Each element was taken to be conductively linked to its eight nearest neighbors, and the spread of depolarization was controlled by a simple conduction scheme in which an element depolarized if two conditions were met: (*i*) the time since its last depolarization exceeded the element's refractory period and (*ii*) one or more of its eight neighboring elements depolarized during the previous time iteration. Conduction velocity, v, was controlled by appropriate scaling of the iteration time t. One iteration per t sec corresponded to a conduction velocity of ξ/t.

The model was activated by exciting (depolarizing) one element of the array at regular intervals T. This element, located at the upper edge of the cylinder, therefore represented the atrioventricular junction. The stimulation rate $r = 1/T$ represented the rate at which the atrioventricular junction conducts impulses to the ventricle. The six adjustable model parameters, therefore, are as follows: ventricular dimension, L; element size, ξ (spatial correlation length of refractory times); mean refractory period, $\bar{\tau}$; standard deviation of refractory period, σ; conduction velocity, v; and stimulation rate, r.

The activity of the model was represented in terms of a simulated ECG obtained in the following way. First, the total cardiac dipole was computed by regarding each interface between depolarized and repolarized elements as a unit dipole and summing the individual dipoles vectorially. The single lead ECGs were then obtained by projecting the total cardiac dipole on a given lead vector axis. This approach is completely analogous to the solid angle solution of the ECG "forward problem" (11).

RESULTS

Because the computer simulations involved thousands of iterations on an array consisting of thousands of elements, it was important to condense the amount of available information into a manageable format. The simulated ECGs were chosen because they allowed for significant data compression and provided a simple interpretation of the behavior of the model based on comparisons to clinical ECGs.

During the "normal" pattern of excitation of the model, a wave of depolarization spreads from the element designated as the atrioventricular junction, over the surface of the cylinder. Then, the elements begin to repolarize after their refractory times elapse. The electrocardiogram corresponding to this normal junctional rhythm is shown in Fig. 4*a*. No *P* waves are present because the model lacks atria. The QRS complex corresponds to the spread of the wave of depolarization, and the *T* wave corresponds to the repolarization phase. Because the effective upstroke and downstroke times of the action potential are equal in this model, the greater width of the *T* wave compared to the QRS complex is entirely attributable to the spatial dispersion of refractory times. The *T* wave was usually inverted compared to the QRS complex, because the model lacks the normal endocardial–epicardial gradient of refractory period duration.

By varying the parameters of the model, a variety of disturbances of heart rhythm could be simulated as shown in Fig. 4. These disturbances are of three main types: (*i*) simple 2:1 or 3:1 conduction blocks in which only every second or third programmed stimulation resulted in depolarization of the bulk of the array; (*ii*) short self-terminating reentrant disturbances; and (*iii*) self-sustaining reentrant rhythms.

In Fig. 4*b* we see an example of a type *i* disturbance in which 2:1 conduction develops. Fig. 4 *c* and *d* shows type *ii* disturbances—short self-terminating reentrant activity. Type *iii* disturbances are shown in Fig. 4 *e* and *f*. Fig. 4*e* resembles the clinical rhythm disturbance, ventricular tachycardia (an organized self-sustained reentrant rhythm), whereas Fig. 4*f* resembles ventricular fibrillation (a chaotic, turbulent pattern of self-sustained reentrant activity).

We systematically probed the electrical stability of the model as a function of programmed stimulated rate ($r = 1/T$), $\bar{\tau}$, σ, and v. In these tests, the values of $\bar{\tau}$, σ, and v were first chosen, and r was set at a level low enough that normal junctional rhythm resulted. Then r was progressively in-

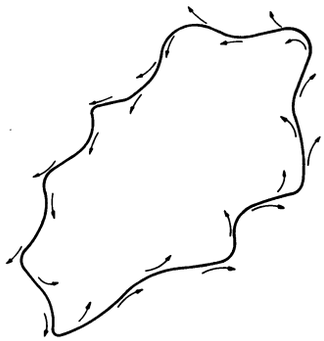

FIG. 2. Condition for self-sustained reentry, $l > v\tau$.

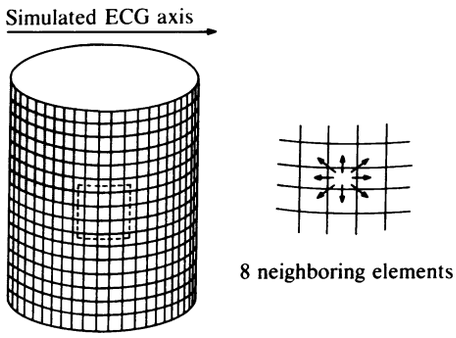

FIG. 3. Cylindrical finite element model for ventricular conduction. Shaded elements are depolarized, unshaded elements are repolarized.

creased in steps of 5 beats per min. At each rate r, the simulated ECG was examined for 20 beats of activity. We defined the critical rate r_c to be the smallest value of r that led to a recognizable disturbance of rhythm of types *i*, *ii*, or *iii*.

In Fig. 5*a*, we plot r_c versus σ for three different values of $\bar{\tau}$ at fixed v. Note that for low values of σ (<100 msec) r_c appears relatively constant, at a rate only slightly greater than $1/\bar{\tau}$. The significance of this rests with the observation that for these low values of σ, the rhythm disturbances seen were most apt to be those of a 2:1 conduction block. For low values of σ, it was not the case that reentrant activity led to an inability of the model array to be periodically stimulated; instead it was merely a case of the stimulation rate exceeding the inverse of the mean refractory period, and therefore the entire array failed to conduct the periodic stimulation every other time.

Note also in Fig. 5*a* that with larger values of σ (>100 msec) there appears to be a gentle decrease in r_c with increasing values of σ. For these larger values of σ, the disturbances were of type *ii* or *iii* but not type *i*. Thus, in this region it was the effect of reentrant activity that determined r_c. Within this region of high standard deviation, type *ii*, or the less serious type of disturbance, was more prevalent with smaller values of σ; the self-sustained disturbances (type *iii*) were more often seen with larger values of σ. The reentrant rhythms seen were of a wide variety of electrocardiographic morphologies.

A plot of r_c versus v is shown in Fig. 5*b* for three values of σ. Note that r_c increases monotonically with v, but that the curve tends to plateau as v increases above 100 cm/sec. For values of v greater than 100 cm/sec, the disturbances were either type *i* or type *ii*. For values of v less than 100 cm/sec, the type of disturbance seen was generally type *iii*. These findings are consistent with the idea that, for reentry to be sustained, the conduction velocity must be low enough that the reentrant wave front does not extinguish itself (Fig. 2).

In Fig. 5*c* we plot r_c versus $\bar{\tau}$ for five values of σ. In what might seem contrary to our intuition regarding reentry in a model such as this, the plots show a nonmonotonic dependence of r_c on $\bar{\tau}$. Indeed, the data suggest that, for a given σ, there is a $\bar{\tau}$ value for which the stability (measured here as r_c) is maximized. This nonmonotonic dependence of r_c on $\bar{\tau}$ is understood when one considers that the evolution of a reentrant rhythm disturbance depends on two separate processes—wave-front fractionation and subsequent reentry. Wave-front fractionation is the process by which a spreading wave front of depolarization impinges on islands of refractory tissue. In the model, this begins to occur when the refractory periods of some of the elements exceed the inter-beat interval (Fig. 6). Thus we see that wave-front fractionation is favored as $\bar{\tau}$ increases. Sustained reentry, on the other hand, is favored by short refractory periods in that shorter reentrant circuits can be sustained as the $\bar{\tau}$ decreases (Fig. 2). At short mean refractory periods, reentrant loop formation is favored and the model is unstable. At long mean refractory periods, wave-front fractionation is favored and again the model is unstable. It is only in the middle ground, in which $\bar{\tau}$ values range from 200 to 250 msec, that stability is maximized. It is intriguing that 200–250 msec corresponds to the approximate duration of the mammalian myocardial cell refractory period.

In the course of systematically examining the electrical stability of the model by varying the parameters of the model (r, $\bar{\tau}$, σ, and v), we made the following observation. The simulated ECGs always showed electrical alternans preceding the onset of type *ii* or type *iii* reentrant rhythm disturbances (for example, see Fig. 4 *b* and *c*). Electrical alternans involves an alternation in QRS or *T*-wave morphology (or both) every other beat. The mechanism for this alternans behavior is shown in Fig. 6; when some myocardial cells have refractory periods that exceed the cycle length (T), there will be a corresponding subpopulation of cells that can at most be activated every second beat. This is reflected in electrical alternans in the ECG. This same process leads to wave-front fractionation and thus predisposes to reentrant ventricular dysrhythmias. Electrical alternans has been reported to precede ventricular dysrhythmias (12). It has also been reported to precede ventricular fibrillation in dogs undergoing coro-

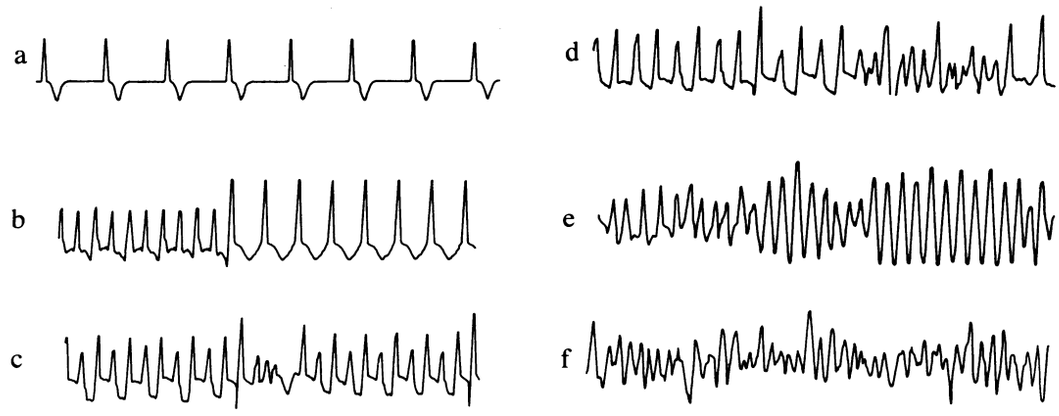

FIG. 4. Simulated ECGs. (*a*) Normal junctional rhythm. (*b*) Development of 2:1 conduction block (type *i* disturbance). (*c*) Three-beat reentrant excitation (type *ii* disturbance). (*d*) Multi-beat self-terminated reentrant activity (type *ii* disturbance). (*e*) Sustained reentrant rhythm that resembles ventricular tachycardia (type *iii* disturbance). (*f*) Disorganized self-sustained reentrant rhythm that resembles ventricular fibrillation (type *iii* disturbance).

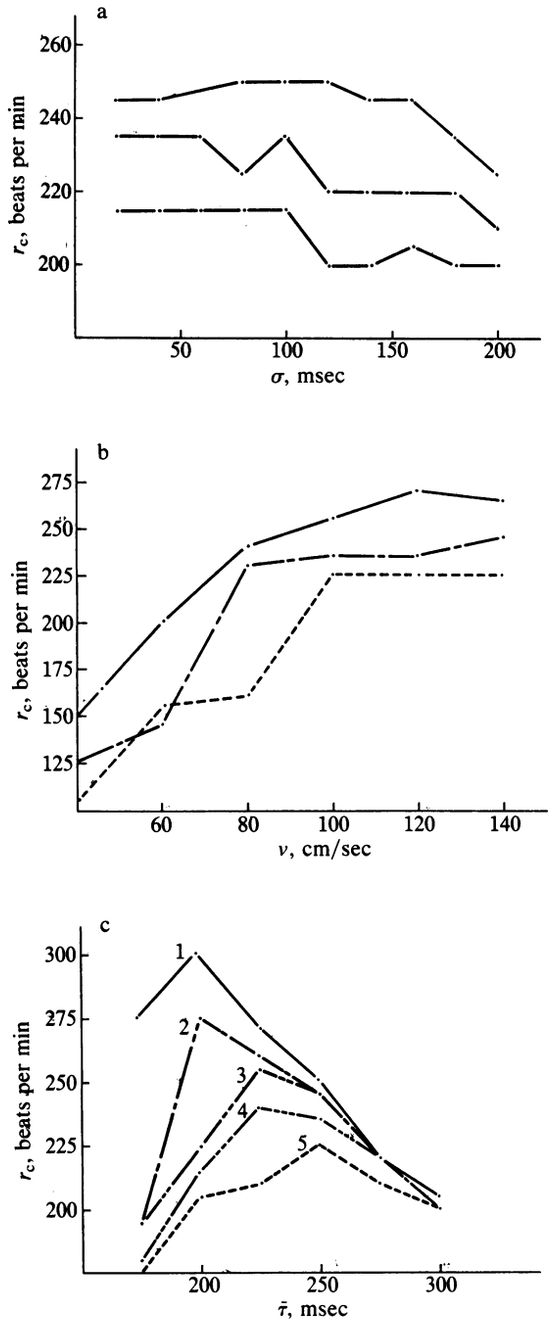

FIG. 5. (*a*) Plot of r_c versus σ for three different values of $\bar{\tau}$ and for v = 100 cm/sec. $\bar{\tau}$ = 250 msec (*Top*); $\bar{\tau}$ = 275 msec (*Middle*); $\bar{\tau}$ = 300 msec (*Bottom*). (*b*) Plot of r_c versus v for three different values of σ and for $\bar{\tau}$ = 250 msec. σ = 150 msec (*Top*); σ = 175 msec (*Middle*); σ = 200 msec (*Bottom*). (*c*) Plot of r_c versus $\bar{\tau}$ for different values of σ and for v = 100 cm/sec. Values of σ are as follows: curve 1, 120 msec; curve 2, 140 msec; curve 3, 160 msec; curve 4, 180 msec; curve 5, 200 msec.

nary artery ligation (13). Canine experiments in our laboratory verify that electrical alternans accompanies decreased electrical stability of the myocardium, whether the intervention be ligation, tachycardia, or hypothermia (14, 15).

DISCUSSION

We have presented a simple finite-element model of ventricular conduction processes incorporating the concept of spatial dispersion of refractoriness. This model purposefully does not incorporate many of the actual electrophysiologic features of ventricular myocardium—for example, no specialized conduction system is present, there is no dependence of local electrical properties (refractory period, conduction velocity) on past local electrical activity, unidirectional blocks are not present, there is no gradation in refractoriness or susceptibility, no pacemaker activity is assumed within the ventricles, the geometry ignores the finite wall thickness, etc.

The purpose of these simulations was to incorporate in a physical model the very minimal features of ventricular conduction needed to represent spatial dispersion of refractoriness, in order to test in a direct way whether spatial dispersion of refractoriness by itself is a sufficient mechanism to generate a variety of reentrant disturbances of rhythm. We found, in fact, that this simple model displays a wide variety of patterns of electrical activity encompassing the spectrum of ventricular rhythm disturbances including ventricular fibrillation. Thus, spatial dispersion of refractoriness may be a sufficient condition to sustain reentrant patterns of activity.

We also investigated the electrical stability of the model as a function of the model parameters $\bar{\tau}$, σ, v, and r. The resulting stability phase diagrams can be qualitatively understood in terms of two processes—wave-front fractionation and subsequent reentry. The first process involves the conditions needed for establishing islands of refractory tissue and the second process involves the sustained recirculation around such barriers. Reentry in this system is formally analogous to a time-dependent percolation process in which activation paths circulate continuously around moving barriers of refractory tissue. Time-dependent percolation theory is analytically difficult. However, preliminary analysis of this system in terms of time-independent percolation models in which one looks for closed paths of length $l > \tau v$ yields results in rough quantitative agreement with the results of the computer simulation (unpublished data).

The observation that electrical alternans precedes the onset of reentrant activity has been used experimentally as a noninvasive measure of electrical stability of the ventricles (14, 15). Electrical alternans in fact represents an excitation of the system at the first subharmonic of r. Recently, such period-doubling phenomena have been shown theoretically and experimentally to be a central feature of a wide variety of systems that approach a chaotic state (16). Thus, the approach to ventricular fibrillation may follow a type of trajectory not dissimilar to that of other systems approaching a disorganized state.

The simple model presented here has permitted the evaluation of the dispersion of refractoriness hypothesis as a sufficient condition for the initiation of reentrant dysrhythmias. The results of this investigation suggest that time-dependent percolation and bifurcation theory may be important concepts in the development of an analytic understanding of the

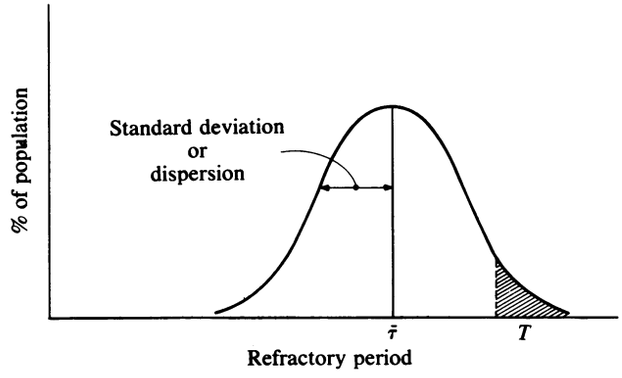

FIG. 6. Probability distribution of refractory periods. Shaded area indicates refractory times that exceed cycle length T.

genesis of reentrant dysrhythmias. It will be important to incorporate into this simple model more of the actual electrophysiologic features of the ventricular conduction system to see how these affect the electrical stability of the system.

This work was supported by National Science Foundation Grant 8121571-ECS, Office of Naval Research Grant N00014-80-C-0520, and a grant from R. J. Reynolds Industries. J.M.S. is grateful for support from an Edward J. Poitras Fellowship, and R.J.C. is grateful for support from a John A. and George L. Hartford Foundation Fellowship.

1. Han, J., de Jalon, P. G. & Moe, G. K. (1964) *Circ. Res.* **14,** 516–524.
2. Han, J., Rheinboldt, W. C. & Abildskov, J. A. (1964) *Am. Heart J.* **67,** 200–220.
3. Han, J., de Jalon, G. & Moe, G. K. (1966) *Circ. Res.* **17,** 18–25.
4. Han, J. (1969) *Am. J. Cardiol.* **24,** 800–812.
5. Moore, E. N. & Speare, J. F. (1975) *Arch. Intern. Med.* **135,** 446–453.
6. Wit, A. L., Hoffman, B. F. & Cranefield, P. F. (1972) *Circ. Res.* **30,** 1–10.
7. Wit, A. L., Hoffman, B. F. & Cranefield, P. F. (1972) *Circ. Res.* **30,** 11–22.
8. Naimi, S., Avitall, B., Mieszala, J. & Levine, H. J. (1977) *Am. J. Cardiol.* **39,** 407–412.
9. Elharrer, V. & Zipes, D. P. (1977) *Am. J. Physiol.* **233,** H329–H345.
10. Moe, G. K., Rheinboldt, W. C. & Abildskov, J. A. (1964) *Am. Heart J.* **67,** 200–220.
11. Plonsey, R. (1969) *Bioelectric Phenomena* (McGraw-Hill, New York), pp. 230–233.
12. Rozanski, J. J. & Kleinfeld, M. (1982) *Pace* **5,** 359–365.
13. Russell, D. C., Smith, H. J. & Oliver, M. D. (1979) *Br. Heart J.* **42,** 88–96.
14. Adam, D. R., Akselrod, S. & Cohen, R. J. (1981) *Comp. Cardiol.* **8,** 307–310.
15. Adam, D. R., Powell, A. O., Gordon, H. & Cohen, R. J. (1982) *Comp. Cardiol.* **9,** 241–244.
16. Feigenbaum, M. J. (1980) *Los Alamos Science*, 4–27.